16th European Signal Processing Conference (EUSIPCO 2008), Lausanne, Switzerland, August 25-29, 2008, copyright by EURASIP

DETECTION OF EPILEPTIC INDICATORS ON CLINICAL SUBBANDS OF EEG

Zeynep Yücel, A. Bülent Özgüler

Electrical and Electronics Engineering, Bilkent University
Bilkent, 06800, Ankara, Turkey
phone: + (90) 312 290 1219, fax: + (90) 312 266 4192, email: zeynep@ee.bilkent.edu.tr
web: www.ee.bilkent.edu.tr/ zeynep

ABSTRACT

Symptoms of epilepsy, which is characterized by abnormal brain electrical activity, can be observed on electroencephalography (EEG) signal. This paper employs models of chaotic measures on standard clinical subbands of EEG and aims to help detection of epilepsy seizures and diagnosis of epileptic indicators in interictal signals.

1. RELATED WORK

Lehnertz divides EEG analysis techniques into two categories, [19], as linear and nonlinear methods. The algorithms described in [11], [17], [15] are regarded as linear methods. Juling et. al., [17] and Jahankhani et. al., [15], consider wavelet based methods to extract time-frequency characteristics of EEG to discriminate between ictal and interictal phases. Among nonlinear analysis techniques neural networks is a widely used approach, [20], [9]. In [8], authors employ short term Lyapunov exponent to classify "normal" and "abnormal" EEG signals. The time evolution of the trajectory is derived from recurrence plots to anticipate seizures in [21]. Hamadene et al., [13], interpret recurrence plots for prediction of epileptic seizures similar to [21]. Entropy related features are used in predicting seizures, [22], detecting patient-specific pre-cursors, [5], and discriminating between seizure and pre-seizure periods, [6]. Independent component analysis [16], phase locked loops [12] and combination of several of the above approaches [23] are among other EEG signal processing techniques.

In this research, we aim to model chaotic measures of a standard subband of EEG and distinguish between different characteristics concerning epilepsy. The outline of the paper is as follows. Section 2 describes the dataset discussed in this work. Section 3 explains details of the proposed method. In Sections 4 and 5, details about the classification schemes, performance rates and conclusions are presented.

2. EEG DATASET

The dataset prepared by the Clinique of Epileptology of Bonn University is utilized in this research, [3]. Single channel EEGs are recorded from people with different brain electrical potential characteristics at a sampling rate of 173.61 Hz for 23.6 sec. These EEG recordings are grouped into three sets denoted by H, E, and S. Set H contains 200 EEG recordings from healthy people, while sets E and S involve recordings from epileptic patients. The 200 recordings in set E are taken in the interictal period, i.e. between seizures. Set S is comprised of 100 recordings in ictal period, i.e. during seizures.

3. METHODOLOGY

The challenge of this research relies on the assumption that the chaotic characteristics of an EEG signal in various frequency bands provide more descriptive information about the physiological condition of the person. In this respect, wavelet transform enables us to handle the signal in different resolution levels and within several frequency bands. Section 3.1 expounds details about standard clinical subbands of EEG and derivation of them by multiresolution analysis. The construction of phase space and derivation of its distinctive chaotic features are explained in Sections 3.2 and 3.3, respectively.

3.1 Standard Clinical Subbands of EEG and Multiresolution Analysis

EEG signals are handled in five standard frequency bands, namely, *delta* $(0-4Hz)$, *theta* $(4-8Hz)$, *alpha* $(8-12Hz)$, *beta* $(13-30Hz)$, and *gamma* $(30-60Hz)$, [2]. Therefore frequencies between $0-60Hz$ provide significant information about the brain electrical potential. Let x_0 be any time series from one of the sets indicated in Section 2. Since x_0 is recorded at a sampling rate of $173.6Hz$, frequencies higher than $60Hz$ appear in its spectral analysis. Obviously a low pass filtering operation is needed to focus on the significant frequency bands. A 10^{th} order Butterworth low pass filter with a suitable cut-off frequency is employed in the extraction of this band.

Herrmann et. al., [14] state that *gamma* activity is closely correlated with cognitive functions and propose that epileptic indicators of EEG are a direct consequence of increase in *gamma* activity. Moreover, Willoughby et. al., [24] show that interictal EEG signals from epileptic patients and healthy people differ enormously in terms of *gamma* activity. Hence, we focus on the *gamma* subband and employ chaotic measures to represent its discriminating characteristics. The *gamma* subband is emphasized by applying a single stage wavelet decomposition using a third order Daubechies filter on the low pass filtered signal. The resulting detail coefficients cover the information in the gamma subband and hence we choose to use such a filter in our analysis.

3.2 Construction of Time Delay Vectors

As a nonlinear dynamical system evolves in time, it could get sufficiently close to a set of states and remain within close neighborhood of that set, even if slightly disturbed. Such states are called attractors. Complexity and chaotic characteristics are the two main descriptors of an attrac-

tor. Complexity is related to geometric properties of the attractor, where chaoticity indicates the rate of divergence or convergence of nearby trajectories in phase space.

As the EEG signal is viewed as the output of a nonlinear dynamical system, it is observed that chaos related features differ between normal and epileptic brain activity. In this research, we focus on the chaotic behavior so as to discriminate between healthy, interictal and ictal EEG. In the analysis of chaotic behavior, recurrence rate is employed as a measure of chaos. The computation of recurrence rate requires formation of time delay vectors. Let x_0 be any time series from one of the sets presented in Section 2 and d_1 be the detail coefficients of x_0. Time delay vectors for d_1 are formed in the following manner.

$$\begin{aligned}&\beta^i_{d_1}(d_0) = \{d_1(i), d_1(i+m_0), \ldots, d_1(i+(d_0-1)m_0)\},\\ &1 \le i \le n_{d_1},\ n_{d_1} = N_{d_1} - (d_0-1)m_0,\end{aligned} \tag{1}$$

where d_0 denotes minimum embedding dimension, m_0 denotes optimum lag and N_{d_1} is the size of the time series d_1.

In order to form time delay vectors, optimum lag m_0 and minimum embedding dimension d_0 need to be determined. Details about calculations of m_0 and d_0 are presented in Sections 3.2.1 and 3.2.2.

3.2.1 Determination of Optimum Lag

Optimum lag is the amount of shift between two portions of the time series, which yields minimum overlapping information. Mutual information function, I, which indicates the amount of mutual dependence between two variables, is employed in the computation of optimum lag. For two discrete random variables X and Y, mutual information function is calculated in the following manner,

$$I(X;Y) = \sum_{y\in Y}\sum_{x\in X} p(x,y) log(\frac{p(x,y)}{p_1(x)p_2(y)}).$$

Let d_1^i contain the data points of d_1 between time instants i and $N_{d_1} - m$. Similarly, d_1^{i+m} contains data points of d_1 between time instants $i+m$ and N_{d_1}:

$$\begin{aligned}d_1^i &= \{d_1(i), d_1(i+1), \ldots d_1(N_{d_1}-m)\},\\ d_1^{i+m} &= \{d_1(i+m), d_1(i+m+1), \ldots d_1(N_{d_1})\}.\end{aligned}$$

We denote the amount of mutual dependence between d_1^i and d_1^{i+m} by $I(m)$. As $I(m)$ is computed for several values of m, the evolution of mutual dependence between two time series with respect to various values of lag can be observed. Obviously, a larger lag leads to little overlapping information, where a smaller lag provides the number of data points in d_1^i and d_1^{i+m} to be large enough to make plausible inferences. Therefore the first local minimum of $I(m)$ is proposed to be the optimum lag m_0, [1].

Figure 1 depicts an example of evolution of mutual information for an element of set S with respect to increasing values of m. Optimum lag is found to be $m_0 = 9$ for this particular time series.

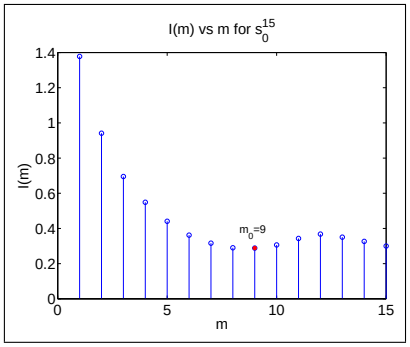

Figure 1: Evolution of Mutual Information for a sample time series from set S

3.2.2 Determination of Minimum Embedding Dimension

Cao describes a requirement for an embedding dimension d to be accepted as a *true* embedding dimension and a method for the calculation of this number, [7]. Assume the time delay vector $\beta^i_{d_1}(d)$ is formed from d_1 using some arbitrary embedding dimension d, as in Equation 1. According to Cao, a true embedding dimension, d_0, satisfies the requirement that two time delay vectors, $\beta^i_{d_1}(d_0)$ and $\beta^j_{d_1}(d_0)$, that lie close to each other in d_0-dimensional space, will still be close to each other in (d_0+1)-dimensional space. In order to investigate whether a certain embedding dimension d fulfills this requirement or not, we check the proximity of two time delay vectors, which are nearest neighbors in d-dimensional space, in $(d+1)$-dimensional space. Let $\beta^{n(i,d)}_{d_1}(d)$ denote the nearest neighbor of $\beta^i_{d_1}(d)$ in d-dimensional space and $a_{d_1}(i,d)$ denote the ratio of distance between these two time delay vectors in d-dimensional to $(d+1)$-dimensional spaces, i.e.,

$$a_{d_1}(i,d) = \frac{\left\|\beta^i_{d_1}(d) - \beta^{n(i,d)}_{d_1}(d)\right\|}{\left\|\beta^i_{d_1}(d+1) - \beta^{n(i,d)}_{d_1}(d+1)\right\|},$$

where $\|.\|$ denotes Euclidean distance. Let $E_{d_1}(d)$ denote the mean value of $a_{d_1}(i,d)$'s:

$$E_{d_1}(d) = \frac{1}{N_{d_1} - dm_0}\sum_{i=1}^{N_{d_1}-dm_0} a_{d_1}(i,d),$$

and $E^1_{d_1}(d)$ be equal to $E_{d_1}(d+1)/E_{d_1}(d)$. $E^1_{d_1}$ is expected to settle around a certain value for embedding dimensions larger than some particular $d_0 - 1$. As a rule of thumb, d_0 is called the minimum embedding dimension. However in practical computations, $E^1_{d_1}$ could yield misleading results due to limited number of elements of phase space. To overcome this problem, Cao redefines the quantification of neighborhood condition by $E^\star_{d_1}(d)$,

$$E^\star_{d_1}(d) = \frac{1}{N - d\tau}\sum_{i=1}^{N-d\tau} \left|d_1(i+d\tau) - d_1(n(i,d))\right|.$$

In this case, the variation between successive embedding dimensions is investigated by $E^2_{d_1} = E^\star_{d_1}(d+1)/E^\star_{d_1}(d)$. The minimum embedding dimension could be calculated

for each time series by applying the same rule of thumb on $E^{\star}_{d_1}$ and a phase space could be constructed accordingly. In such a case, the number of time delay vectors contributing to the phase space from a particular time series will be $N_{d_1} - m_0(d_0 - 1)$.

Here one should note that, although N_{d_1} is fixed in our case, m_0 and d_0 can change the number of constructed time delay vectors pretty much. In order to have a fair comparison, it is preferred to calculate a separate m_0 for each d_1 and to keep d_0 fixed. To determine the optimum constant for minimum embedding dimension, we calculate d_0's for all possible time series d_1 and pick the one which is most voted. It is observed that $d_0 = 7$ is the minimum embedding dimension for most of the time series.

3.3 Modeling Recurrence Rate Behavior

After determining optimum lag and minimum embedding dimension, one can construct time delay vectors for each *gamma* subband as in Equation 1. The collection of time delay vectors form a lagged phase space with elements $\beta^i_{d_1}(d_0)$. The discriminative features of a particular EEG recording x_0 is derived from the recurrence properties of this lagged phase space.

Section 3.3.2 gives details about modeling recurrence rate and describes the derivation of feature vectors. The distribution of feature vectors is illustrated in Section 3.3.3.

3.3.1 Measures of Chaoticity and Recurrence Plots

Chaos can be measured by correlation dimension, recurrence rate, determinism percentage, Hurst exponent, or largest Lyapunov exponent, [18], among other methods. Here we make use of recurrence rate. Any two states, which lie in some proximity smaller than ε, are called recurrence states. Recurrence plot is a graphical tool to visualize the recurrence states and recurrence rate is a simple recurrence quantifier derived from the recurrence plot.

Let $\mathbf{R}$ denote the $N \times N$ recurrence plot of a phase space with elements σ_i, where $1 \leq i \leq N$, as N denotes the number of elements of the phase space. The value of a point (i, j) on the recurrence plot $\mathbf{R}$ is computed by the following equation,

$$\mathbf{R}(i,j) = \Theta(\varepsilon - \|\sigma_i - \sigma_j\|),$$

where Θ is the Heaviside step function and ε is the distance threshold. It is obvious from the above equation, that if there are any two states in the phase space, σ_i and σ_j, which are in some proximity smaller than ε, the value of $\mathbf{R}(i,j)$ is 1 and otherwise 0. Figure 2 presents two recurrence plots of a sample time series from set H for $\varepsilon = 15$ and $\varepsilon = 20$ cases. As expected increasing the threshold makes the neighborhood condition looser and hence number of recurrence points increases.

3.3.2 Recurrence Quantification and Derivation of Feature Vectors

In recurrence quantification, recurrence rate Ψ, which basically denotes the density of recurrence points in $\mathbf{R}$, is employed.

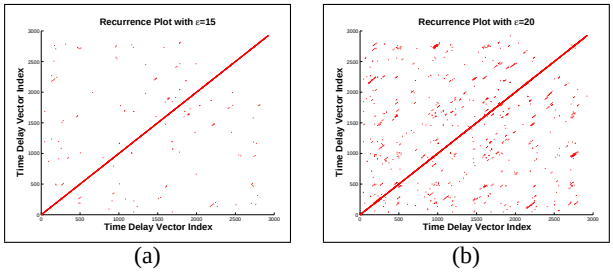

(a) (b)

Figure 2: Recurrence plots of a sample time series from set H for (a) $\varepsilon = 15$ and (b) $\varepsilon = 20$.

$$\Psi = \frac{1}{N^2} \sum_{i,j=1}^{N} \mathbf{R}(i,j).$$

Feature vectors are derived by examining the evolution of recurrence rate against different values of distance threshold. For a particular distance threshold, ε_k, the recurrence rate of lagged phase space of time series d_1 is given by

$$\Psi^k_{d_1} = \frac{1}{N^2_{d_1}} \sum_{\substack{i,j=1 \\ i \neq j}}^{N_{d_1}} \Theta(\varepsilon_k - \left\| \beta^i_{d_1}(d_0) - \beta^j_{d_1}(d_0) \right\|).$$

To observe the evolution of recurrence rate against distance threshold, we calculate $\Psi^k_{d_1}$ for various values of $\varepsilon_k \in \{\varepsilon_1, \varepsilon_2, ..., \varepsilon_K\}$ and obtain a series of recurrence rates, $\Psi_{d_1} = \{\Psi^1_{d_1}, \Psi^2_{d_1}, ..., \Psi^K_{d_1}\}$. As seen in Figure 3-(a), these series are observed to exhibit a different nature for sets H, E and S and therefore could be used to represent features. However, using raw recurrence rate series is not handy, since the size of Ψ_{d_1} could be large depending on the number of distance thresholds, K. In order to provide a dimension reduction, a simple model is developed for Ψ_{d_1} such that the feature vector of a particular time series d_1 is composed of the parameters of the adopted model for Ψ_{d_1}.

After examining the graph of $\Psi^k_{d_1}$ against ε_k, it is observed that it exhibits almost a linear increase for certain values of ε_k. Moreover, it is clear from Figure 3 that the linear regions have different slopes in general and occur mostly at different values of ε_k for sets H, E and S. Thus the

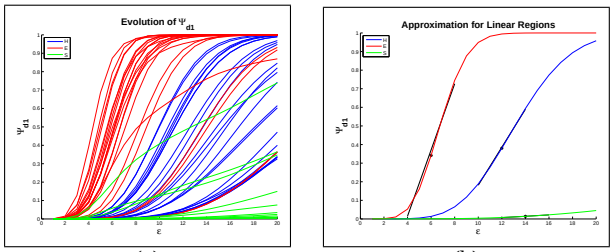

(a) (b)

Figure 3: (a) Evolution of $\Psi^k_{d_1}$ against ε_k for several sample time series, (b) Approximations for the linear regions.

evolution of Ψ_{d_1} can be represented using the parameters of

the linear approximation $a_0\varepsilon + b_0$ and the value of distance threshold ε_0 at the center of the linear region. In this manner, parameters a_0, b_0 and ε_0 are assumed to summarize the evolution of Ψ_{d_1} with respect to distance threshold and are considered to provide a distinction.

3.3.3 Distribution of Feature Vectors

After determining a model for the evolution of recurrence rate and solving for the model parameters, we should check whether these parameters provide a distinction between underlying brain electrical potentials. Figure 4 depicts the distribution of parameters a_0, b_0 and ε_0 for sets H, E, S and verifies that the parameters occupy mostly different regions.

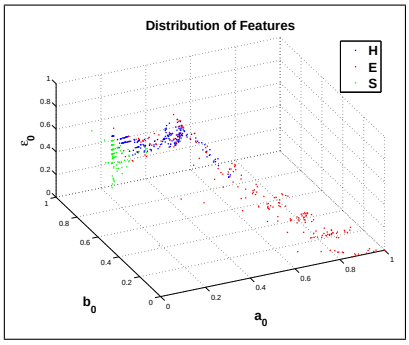

Figure 4: Distribution of features

4. CLASSIFICATION

K-nearest neighbor classification is employed in discriminating the physiological differences between the scalp EEG recordings described in Section 2. This section is dedicated to the details of the classification scheme. Section 4.1 explains the cross-correlation schemes used in the testing and training of linear discriminant classifier. Performance rates are presented in Section 4.2. Comparison with the existing techniques is handled in Section 4.3.

4.1 Cross-Correlation Scheme

The test performance is investigated via a series of classification experiments. Test performance shows how well the classifier performs when new patterns are investigated for class membership. While measuring test performance, the classifier is trained with a number of training patterns and then tested by new patterns. The number of training patterns is increased step by step and the classifier is tested by the rest of the dataset at each step. As we increase the number of training examples, we expect to see the classification performance to increase and settle down around a steady state value. In this manner, we can see how large a data set suffices to describe the classes thoroughly.

The graphs below show the success rates while number of training samples is increased from 5 to 70. For each case ten experiments are made. The solid line shows the mean of those, while the vertical ones indicate their maximum and minimum.

4.2 Test Performance

From Figure 5, it is observed that the classifier performs better in distinction of sets H and S. As number of training samples gets over 20, success rates reach 88% and 94% respectively. For the set E, performance is around 72% regardless of the number of training samples.

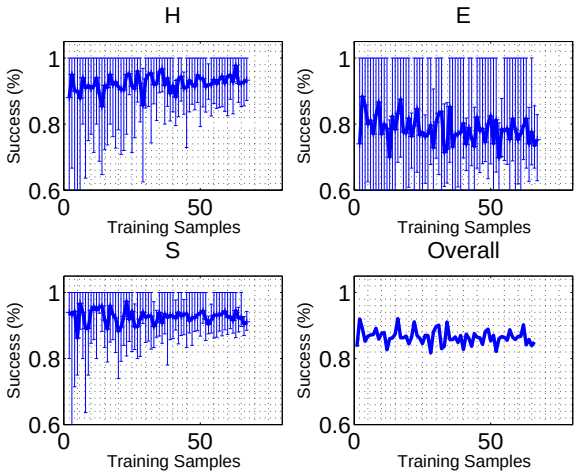

Figure 5: Evolution of success rate in testing

4.3 Comparison with Existing Techniques

Andrzejak provides a list of papers which use the same dataset in analysis and classification of EEG signals, [4]. Most of these papers consider different groups of EEG signals by either eliminating some classes, dividing some classes into further sub-classes or formulate a different problem by comparing the symptoms of epilepsy to symptoms of other physiological disorders. Among these papers, [10] and [1] consider a similar problem formulation to ours. Our scheme employs a phase space, which is built similar to the one in [1], however, we introduce the modeling of recurrence rate of the phase space and classification using the model parameters unlike [1]. Gautama et. al. [10] treat the same problem considered in this work by employing delay vector variance (DVV) method. They achieve 74.4% overall success rate. With our method, overall success rate is always around 85% as seen in Figure 5. Thus our method outperforms DVV in overall performance.

5. CONCLUSION

In this paper, we propose a method for discrimination of EEG recordings from people with different epileptic characteristics. A model is developed for the recurrence rate derived from *gamma* band of the EEG signals. It is shown to exhibit different natures for healthy, ictal and interictal cases. The proposed classification scheme performs well for healthy and ictal EEGs but only fairly good for interictal EEGs and needs to be improved. As a future work, we will consider applying hierarchical classification with a more effective classifier. Moreover, the multiresolution analysis could be improved by employing a filterbank which results in less aliasing than the Daubechies wavelets.

REFERENCES

[1] Adeli, H., Ghosh-Dastidar, S., Dadmehr, N., "A Wavelet-Chaos Methodology for Analysis of EEGs and EEG Subbands to Detect Seizure and Epilepsy", *IEEE Transactions on Biomedical Engineering*, Volume 54, Issue 2, Feb. 2007, Page(s):205 - 211.

[2] Assaleh, K., Al-Nashash, H., Thakor, N., "Spectral Subtraction and Cepstral Distance for Enhancing EEG Entropy", *Engineering in Medicine and Biology Society, 2005. IEEE-EMBS 2005. 27th Annual International Conference of the*, 2005, 2751-2754.

[3] Andrzejak, R. G., Lehnertz, K., Mormann, F., Rieke, C., David, P., Elger, C.E., "Indications of Nonlinear Deterministic and Finite-Dimensional Structures in Time Series of Brain Electrical Activity: Dependence on Recording Region and Brain State", P*hys. Rev. E*, Volume 64, No 6, Nov. 2001, Pages 061907-8.

[4] Klinik für Epileptologie, *http://www.meb.uni-bonn.de/epileptologie/cms/frontcontent.php*

[5] D'Alessandro, M., Esteller, R., Vachtsevanos, G., Hinson, A., Echauz, J., Litt, B., "Epileptic seizure prediction using hybrid feature selection over multiple intracranial EEG electrode contacts: a report of four patients", *IEEE Transactions on Biomedical Engineering*, Volume 50, Issue 8, Aug. 2003 Page(s):1041 - 1041.

[6] Bianchi, A.M., Panzica, F., Tinello, F., Franceschetti, S., Cerutti, S., Baselli, G., "Analysis of multichannel EEG synchronization before and during generalized epileptic seizures", *Proceedings of First International IEEE EMBS Conference on Neural Engineering*, 20-22 March 2003, Page(s):39 - 42

[7] Cao, L., "Practical Methods for Determining The Minimum Embedding Dimension of a Scalar Time Series". *Physica D*, 1997, Page(s) 43-50.

[8] Chaovalitwongse W. A. , Fan Y.-J. , Sachdeo R. C. , "On the Time Series K-Nearest Neighbor Classification of Abnormal Brain Activity", *IEEE Transactions on Systems and Man and Cybernetics-Part A: Systems and Humans:Accepted for future publication*, Issue 99, 2007.

[9] Fischer, P., Tetzlaff, R., "Pattern detection by cellular neuronal networks (CNN) in long-term recordings of a brain electrical activity in epilepsy", *Proceedings of IEEE International Joint Conference on Neural Networks*, 2004, Volume 1, 25-29 July 2004.

[10] Gautama, T., Mandic, D.P., Van Hulle, M.M., "Indications of nonlinear structures in brain electrical activity", *Physical Review E*, Volume 67, Issue 4, April 2003.

[11] Güler, I., Kiymik, M.K., Akin, M., Alkan A., "AR Spectral Analysis of EEG Signals by Using Maximum Likelihood Estimation", *Computers in Biology and Medicine*, Volume 31, 2001, pp. 441-450.

[12] Gysels, E., Le Van Quyen, M., Martinerie, J., Boon, P., Vonck, K., Lemahieu, I., Van De Walle, R., "Long-term evaluation of synchronization between scalp EEG signals in partial epilepsy", *Proceedings of the* 9^{th} *International Conference on Neural Information Processing, 2002. ICONIP '02.* , Volume 3, 18-22 Nov. 2002 Page(s):1495 - 1498.

[13] Hamadene, W., Peyrodie, L., Seidiri, H., "Interpretation of RQA variables: Application to the prediction of epileptic seizures", *The* 8^{th} *International Conference on Signal Processing*, Volume 4, 16-20 2006.

[14] Herrmann, C.S., Demiralp, T., "Human EEG gamma oscillations in neuropsychiatric disorders", *Clinical Neurophysiology*, Volume 116, 2005, Page(s): 2719-2733.

[15] Jahankhani, P., Revett, K., Kodogiannis, V., "Data Mining an EEG Dataset with an Emphasis on Dimensionality Reduction", *IEEE Symposium on Computational Intelligence and Data Mining, 2007, CIDM 2007*, March 1 2007-April 5 2007 Page(s):405 - 412.

[16] James, C.J., Lowe, D.,"Using independent component analysis & dynamical embedding to isolate seizure activity in the EEG", *Proceedings of the* 22^{nd} *Annual International Conference of the IEEE Engineering in Medicine and Biology Society, 2000*, Volume 2, 23-28 July 2000 Page(s):1329 - 1332.

[17] Junling, Z., Dazong, J., "A linear epileptic seizure predictor based on slow waves of scalp EEGs", 27^{th} *Annual International Conference of the Engineering in Medicine and Biology Society, 2005, IEEE-EMBS 2005*, 01-04 Sept. 2005, Page(s):7277 - 7280.

[18] Kannathal, N., Acharya, U. R., Lim, C.M., Sadasivan, P. K., "Characterization of EEG-A comperative study", *Computer Methods and Programs in Biomedicine*, 2005, Page(s) 17-23.

[19] Lehnertz, K., "Seizure prediction techniques: robustness and performance issues", *Proceedings of the Second Joint EMBS/BMES Conference, 2002*, Volume 3, 23-26 Oct. 2002, Page(s):2037 - 2038.

[20] Niederhoefer, C., Tetzlaff, R.,, "Prediction Error Profiles allowing a Seizure Forecasting in Epilepsy? ", 10^{th} *International Workshop on Cellular Neural Networks and Their Applications, 2006. CNNA '06*, 28-30 Aug. 2006 Page(s):l - 6.

[21] Ouyang, G., Xie, L., Chen, H., Li, X., Guan, X., Wu, H., "Automated Prediction of Epileptic Seizures in Rats with Recurrence Quantification Analysis", 27^{th} *Annual International Conference of the Engineering in Medicine and Biology Society, IEEE-EMBS 2005*, 2005, Page(s):153 - 156.

[22] Srinivasan, V., Eswaran, C., Sriraam, N., "Approximate Entropy-Based Epileptic EEG Detection Using Artificial Neural Networks", *IEEE Transactions on Information Technology in Biomedicine*, Volume 11, Issue 3, May 2007, Page(s):288 - 295.

[23] Qu, H., Gotman, J.,"A patient-specific algorithm for the detection of seizure onset in long-term EEG monitoring: possible use as a warning device", *IEEE Transactions on Biomedical Engineering*, Volume 44, Issue 2, Feb. 1997 Page(s):ll5 - 122.

[24] Willoughby, J.O., Fitzgibbon, S.P., Pope, K.J., Mackenzie, L., Medvedev, A.V., Clark, C.R., Davey, M.P., Wilcox, R.A., "Persistent abnormality detected in the non-ictal electroencephalogram in primary generalized epilepsy", *Journal of Neurology Neurosurgery and Psychiatry*, 2003, 74:51-55.